



Supplement of

Spatiotemporal Intertropical Convergence Zone dynamics during the last 3 millennia in northeastern Brazil and related impacts in modern human history

Giselle Utida et al.

Correspondence to: Giselle Utida (giselleutida@hotmail.com)

The copyright of individual parts of the supplement might differ from the article licence.

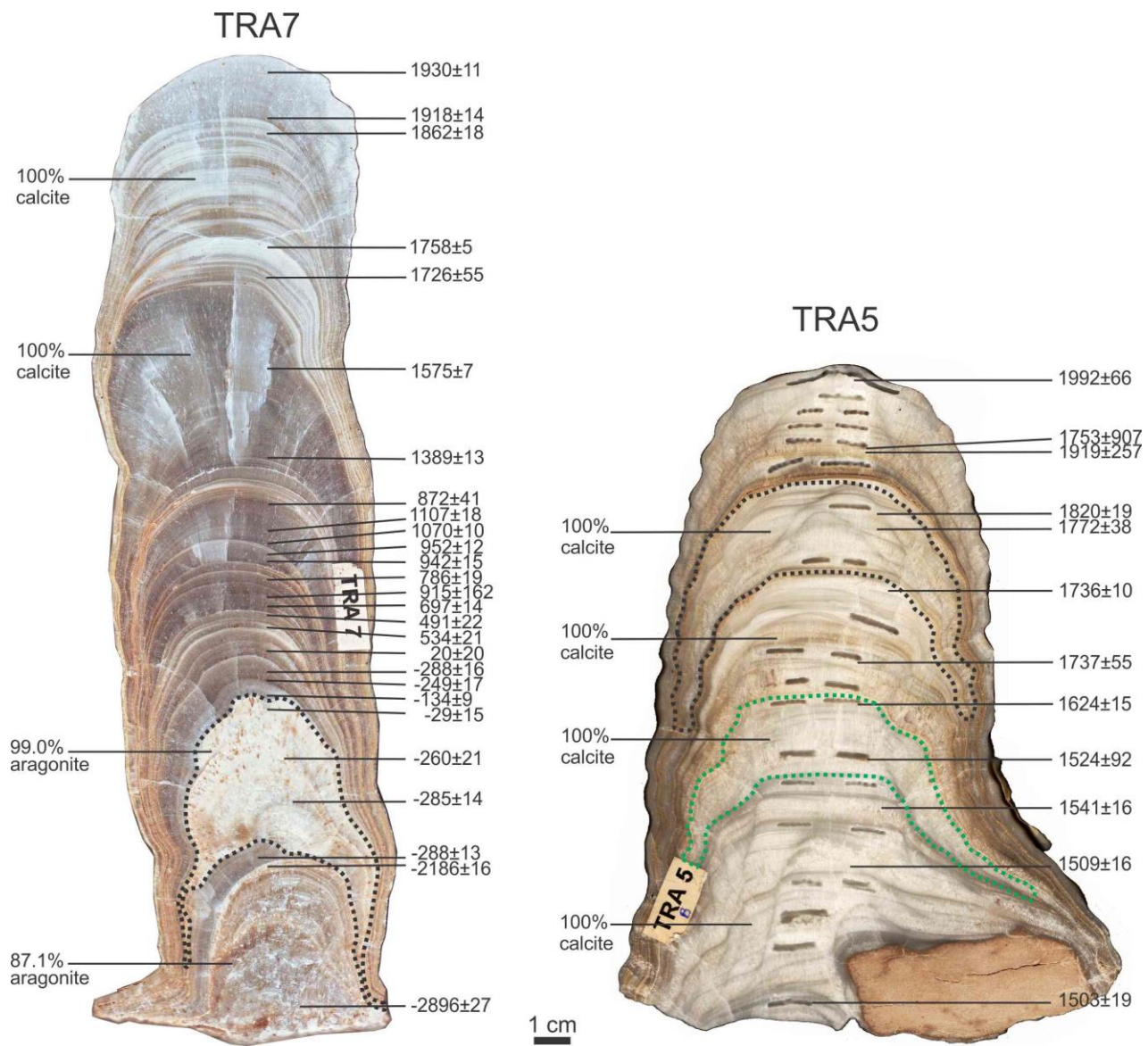
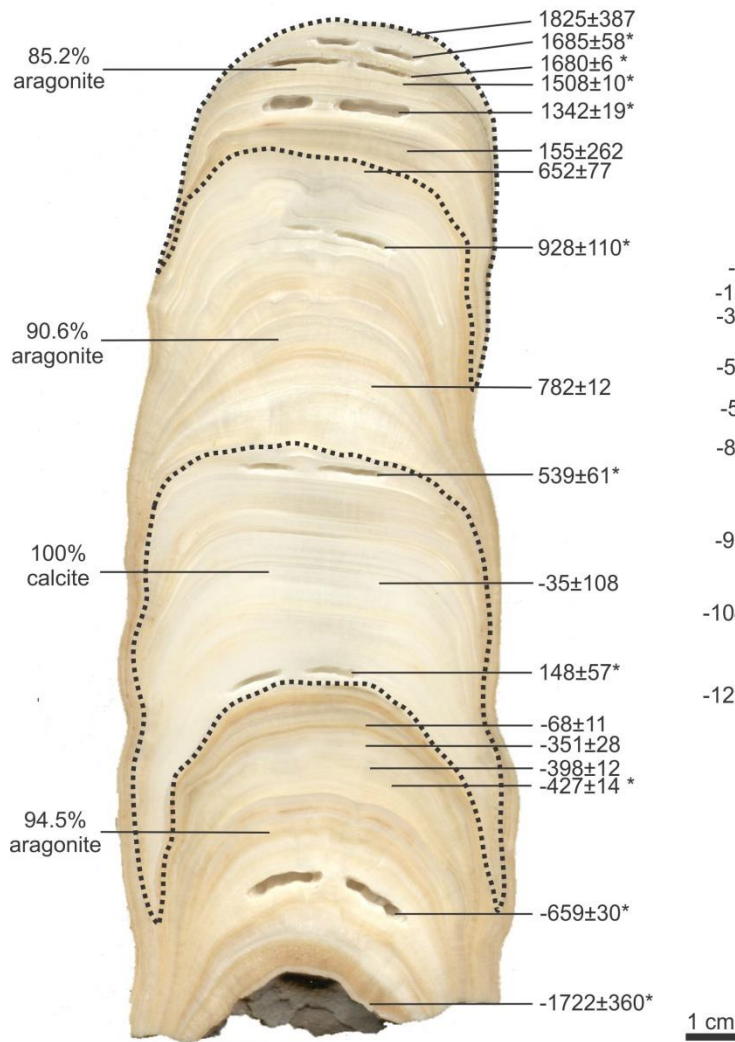


Figure S1 – TRA7 and TRA5 speleothem images indicating results of U/Th ages in BCE/CE and mineralogical composition. Outlines indicate the portions according to mineralogy. TRA7 ages and mineralogy obtained by Utida et al. (2020).

FN1



FN2

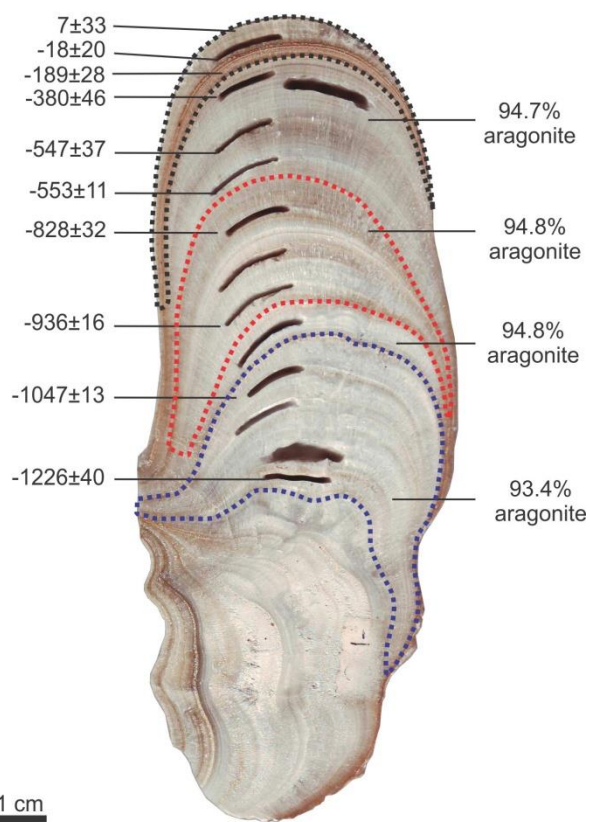


Figure S2 – Speleothem FN1 and FN2 images indicating results of U/Th ages BCE/CE. Outlines indicate the portions according to mineralogy. * FN1 ages obtained by Cruz et al. (2009). FN1 mineralogy obtained by Utida et al. (2020).

Table S1 – Chronological results. U/Th results obtained from speleothem FN1 and FN2. ¹Data obtained by Cruz et al. (2009).

Sample	Depth	²³⁸ U		²³² Th		²³⁰ Th / ²³² Th		^d ²³⁴ U*	²³⁰ Th / ²³⁸ U		²³⁰ Th Age (yr)		²³⁰ Th Age (yr)		^δ ²³⁴ U _{Initial} **	²³⁰ Th Age (yr BP)***		Age BCE/CE		
Number	(mm)	(ppb)		(ppt)		(atomic x10 ⁻⁶)	(measured)	(activity)		(uncorrected)	(corrected)	(corrected)	(corrected)	(corrected)	(corrected)	(corrected)				
FN1 speleothem																				
FN1-1	1	214	± 1	3825	± 18	5.8	±2	-60	±4	0.0064	±0.00232	739	±271	183	±387	-60	±4	125	±387	1825
FN1-a¹	5	119	± 0	228	± 2	28	±4	-68	±3	0.0033	±0.00043	383	±50	323	±58	-68	±3	265	±58	1685
FN1-b¹	9	4134	± 16	698	± 2	280	±5	-58	±1	0.0029	±0.00005	333	±6	328	±6	-58	±1	270	±6	1680
FN1-B1¹	12	7837	± 26	3878	± 10	148	±2	-58	±2	0.0044	±0.00006	515	±7	500	±10	-58	±2	442	±10	1508
FN1-T¹	16	1152	± 4	1256	± 3	91	±1	-61	±2	0.0060	±0.00007	700	±9	666	±19	-61	±2	608	±19	1342
FN1-22	22	701	± 2	8378	± 169	26	±1	-58	±2	0.0191	±0.00013	2234	±17	1864	±262	-58	±2	1795	±262	155
FN1-T2	29	812	± 1	2425	± 49	69	±2	-56	±1	0.0125	±0.00034	1453	±40	1360	±77	-57	±1	1298	±77	652
FN1-2¹	41	48	± 0	151	± 2	54	±5	-53	±2	0.0102	±0.00089	1180	±100	1080	±110	-53	±2	1022	±110	928
FN1-2A	72	5814	± 36	1171	± 6	868	±7	-57	±4	0.0106	±0.00009	1232	±12	1226	±12	-57	±4	1168	±12	782
FN1-3¹	88	85	± 0	209	± 1	90	±3	-56	±2	0.0133	±0.00041	1545	±48	1469	±61	-56	±2	1411	±61	539
FN1-106	106	508	± 1	2506	± 50	63	±1	-52	±2	0.0190	±0.00014	2205	±16	2054	±108	-52	±2	1985	±108	-35
FN1-4¹	127	75	± 0	97	± 1	210	±7	-53	±3	0.0164	±0.00046	1899	±54	1860	±57	-53	±3	1802	±57	148
FN1-4.1	137	13580	± 49	2593	± 53	1535	±31	-62	±2	0.0178	±0.00008	2086	±10	2080	±11	-62	±2	2018	±11	-68
FN1-140	140	12302	± 97	9588	± 208	433	±9	-57	±3	0.0205	±0.00017	2394	±22	2370	±28	-57	±3	2301	±28	-351
FN1-4.2	145	15185	± 51	4074	± 82	1271	±26	-57	±2	0.0207	±0.00008	2418	±10	2410	±12	-57	±2	2348	±12	-398
FN1-4A¹	147	17533	± 81	3486	± 7	1734	±6	-55	±2	0.0209	±0.00011	2441	±14	2435	±14	-56	±2	2377	±14	-427
FN1-B¹	187	20240	± 200	2847	± 8	2680	±12	-55	±3	0.0229	±0.00024	2671	±30	2667	±30	-55	±3	2609	±30	-659
FN1-4B¹	202	7297	± 22	165820	± 830	27	±1	-52	±2	0.0377	±0.00076	4435	±91	3730	±360	-52	±2	3672	±360	-1722
FN2 speleothem																				
FN2-1	1	4480	± 13	7017	± 142	197	±4	-1	±2	0.0187	±0.00007	2058	±8	2012	±33	-1	±2	1943	±33	7
FN2-4	4	5566	± 15	4344	± 12	392	±3	-4	±2	0.0185	±0.00000	2052	±16	2030	±20	-4	±2	1968	±20	-18
FN2-6	6	5161	± 31	5881	± 123	294	±6	0	±3	0.0203	±0.00013	2241	±16	2208	±28	0	±3	2139	±28	-189
FN2-2	10	4525	± 17	9648	± 196	172	±4	1	±2	0.0223	±0.00010	2454	±14	2392	±46	1	±2	2330	±46	-380
FN2-20	20	6588	± 15	11520	± 232	222	±5	-4	±2	0.0236	±0.00008	2610	±10	2559	±37	-4	±2	2497	±37	-547
FN2-27	27	8524	± 23	1698	± 35	1918	±39	-5	±2	0.0232	±0.00008	2571	±10	2565	±11	-5	±2	2503	±11	-553
FN2-3	45	4895	± 20	6182	± 126	338	±7	-2	±2	0.0259	±0.00010	2867	±18	2830	±32	-2	±2	2768	±32	-818
FN2-52	52	9454	± 30	3965	± 80	1041	±21	-11	±2	0.0265	±0.00010	2960	±13	2948	±16	-11	±2	2886	±16	-936
FN2-74	74	16129	± 50	3438	± 70	2131	±43	-6	±2	0.0275	±0.00009	3065	±12	3059	±13	-6	±2	2997	±13	-1047
FN2-6	90	21367	± 213	2993	± 17	3410	±23	-11	±6	0.0289	±0.00031	3242	±40	3238	±40	-11	±6	3176	±40	-1226

U decay constants: $\lambda_{238} = 1.55125 \times 10^{-10}$ (Jaffey et al., 1971) and $\lambda_{234} = 2.82206 \times 10^{-6}$ (Cheng et al., 2013). Th decay constant: $\lambda_{230} = 9.1705 \times 10^{-6}$ (Cheng et al., 2013). * $\delta^{234}\text{U} = ([^{234}\text{U}/^{238}\text{U}]_{\text{activity}} - 1) \times 1000$. ** $\delta^{234}\text{U}_{\text{initial}}$ was calculated based on ²³⁰Th age (T). i.e.. $\delta^{234}\text{U}_{\text{initial}} = \delta^{234}\text{U}_{\text{measured}} \times e^{\lambda^{234}\text{UT}}$. Corrected ²³⁰Th ages assume the initial ²³⁰Th/²³²Th atomic ratio of $4.4 \pm 2.2 \times 10^{-6}$. Those are the values for a material at secular equilibrium. with the bulk earth ²³²Th/²³⁸U value of 3.8. The errors are arbitrarily assumed to be 50%. ***B.P. stands for "Before Present" where the "Present" is defined as the year 1950 A.D.

Table S2 – Chronological results. U/Th results obtained from speleothem TRA5.

Sample	Depth	^{238}U		^{232}Th		$^{230}\text{Th} / ^{232}\text{Th}$		$d^{234}\text{U}^*$	$^{230}\text{Th} / ^{238}\text{U}$		$^{230}\text{Th Age (yr)}$		$^{230}\text{Th Age (yr)}$		$\delta^{234}\text{U}_{\text{Initial}}^{**}$	$^{230}\text{Th Age (yr BP)}^{***}$		Age		
Number	(mm)	(ppb)	(ppt)	(atomic $\times 10^{-6}$)		(measured)	(activity)	(activity)	(uncorrected)	(corrected)	(corrected)	(corrected)	(corrected)	(corrected)	(corrected)	(corrected)	BCE/CE			
TRA5 speleothem																				
TRA5-2	7	1411	± 2	3788	± 76	6	± 1	-145	± 2	0.0009	± 0.00009	119	± 12	27	± 66	-145	± 2	-42	± 66	1992
TRA5-18	18	2035	± 4	76686	± 1543	5	± 0	-139	± 2	0.0121	± 0.00019	1541	± 25	259	± 907	-139	± 2	197	± 907	1753
TRA5-20	20	1915	± 4	20400	± 410	6	± 0	-145	± 2	0.0036	± 0.00010	463	± 12	100	± 257	-145	± 2	31	± 257	1919
TRA5b-37	37	1977	± 2	612	± 13	89	± 8	-139	± 1	0.0017	± 0.00014	211	± 18	200	± 19	-139	± 1	130	± 19	1820
TRA5-41	41	1889	± 5	2858	± 58	25	± 1	-138	± 2	0.0023	± 0.00008	291	± 10	240	± 38	-138	± 2	178	± 38	1772
TRA5-58	58	1921	± 3	585	± 12	122	± 4	-142	± 2	0.0022	± 0.00006	286	± 7	276	± 10	-142	± 2	214	± 10	1736
TRA5-71	71	2371	± 14	5165	± 108	21	± 1	-147	± 5	0.0028	± 0.00012	356	± 16	282	± 55	-147	± 5	213	± 55	1737
TRA5b-90	90	2031	± 2	256	± 6	413	± 18	-139	± 1	0.0032	± 0.00011	401	± 14	396	± 15	-139	± 1	326	± 15	1624
TRA5-104	104	2018	± 14	7328	± 155	22	± 1	-141	± 6	0.0049	± 0.00023	618	± 29	495	± 92	-141	± 6	426	± 92	1524
TRA5-116	116	1785	± 4	912	± 18	124	± 4	-139	± 2	0.0038	± 0.00008	488	± 10	471	± 16	-139	± 2	409	± 16	1541
TRA5-132	132	2699	± 5	1549	± 31	118	± 3	-140	± 2	0.0041	± 0.00006	522	± 8	503	± 16	-140	± 2	441	± 16	1509
TRA5b-169	169	1969	± 2	108	± 5	1237	± 73	-136	± 1	0.0041	± 0.00015	519	± 19	517	± 19	-136	± 1	447	± 19	1503

U decay constants: $\lambda_{238} = 1.55125 \times 10^{-10}$ (Jaffey et al., 1971) and $\lambda_{234} = 2.82206 \times 10^{-6}$ (Cheng et al., 2013). Th decay constant: $\lambda_{230} = 9.1705 \times 10^{-6}$ (Cheng et al., 2013). * $\delta^{234}\text{U} = ([^{234}\text{U}/^{238}\text{U}]_{\text{activity}} - 1) \times 1000$. ** $\delta^{234}\text{U}_{\text{initial}}$ was calculated based on ^{230}Th age (T). i.e.. $\delta^{234}\text{U}_{\text{initial}} = \delta^{234}\text{U}_{\text{measured}} \times e^{\lambda_{234} \times T}$. Corrected ^{230}Th ages assume the initial $^{230}\text{Th}/^{232}\text{Th}$ atomic ratio of $4.4 \pm 2.2 \times 10^{-6}$. Those are the values for a material at secular equilibrium. with the bulk earth $^{232}\text{Th}/^{238}\text{U}$ value of 3.8. The errors are arbitrarily assumed to be 50%. ***B.P. stands for “Before Present” where the “Present” is defined as the year 1950 A.D.

1 Table S3 – Parameters used to establish the composite record of Trapiá and Furna Nova
 2 stalagmites with *iscam* programming (Fohlmeister. 2012)

Parameter	Range	Description
nrAR1	2000	Number of AR1 simulations
nrAR1_MC	1000	Number of MC runs for each AR1
nrMC	100000	Number of MC simulations for measured data sets
nrSMOOTH	10	Number of years used for smoothing before the correlation
CUT	1	Extrapolation of isotope data allowed beyond dated depths
GAUSS	0	MC simulations with Gaussian distribution
Interpol	-1	Pointwise linear interpolation between dated depths
Detrend	2	Detrending and normalizing before running the method

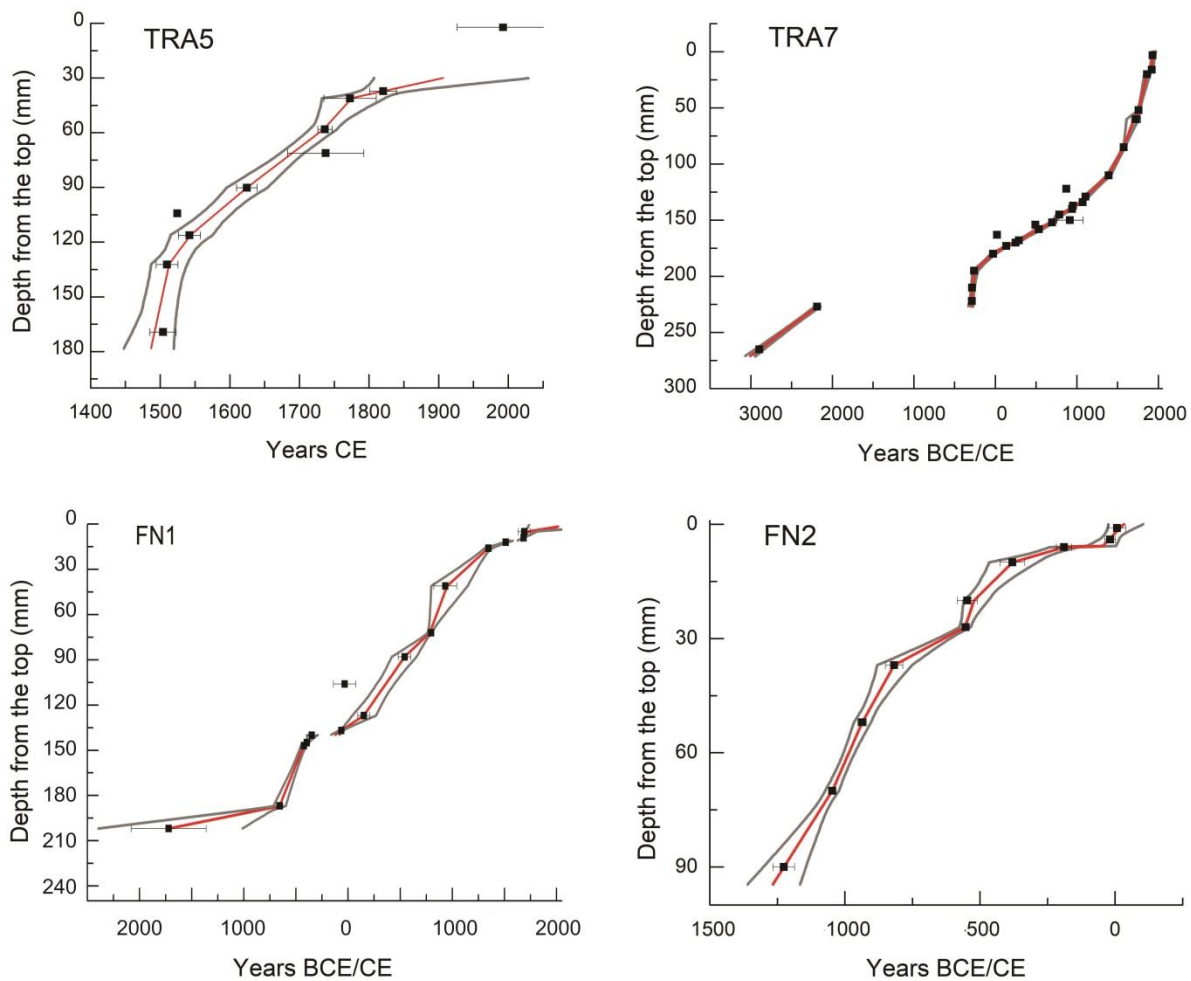
3
 4 Calcite-Aragonite fractionation

5 We use the aragonite-calcite fractionation offset described by Zhang et al. (2014) obtained
 6 for stalagmites from China. We used the equation 1 below to consider the proportion between
 7 calcite and original aragonite for each stalagmite interval of RN stalagmites, according to the Table
 8 S3. We included the mean $\delta^{18}\text{O}$ for each interval before and after C-A correction in Table S3.

9
 10
$$\delta^{18}\text{O}_{\text{C-A corr}} = \frac{\text{sample calcite \%}}{100\% \text{ original aragonite}} \times \text{calcite fractionation offset} \quad \text{Equation (1)}$$

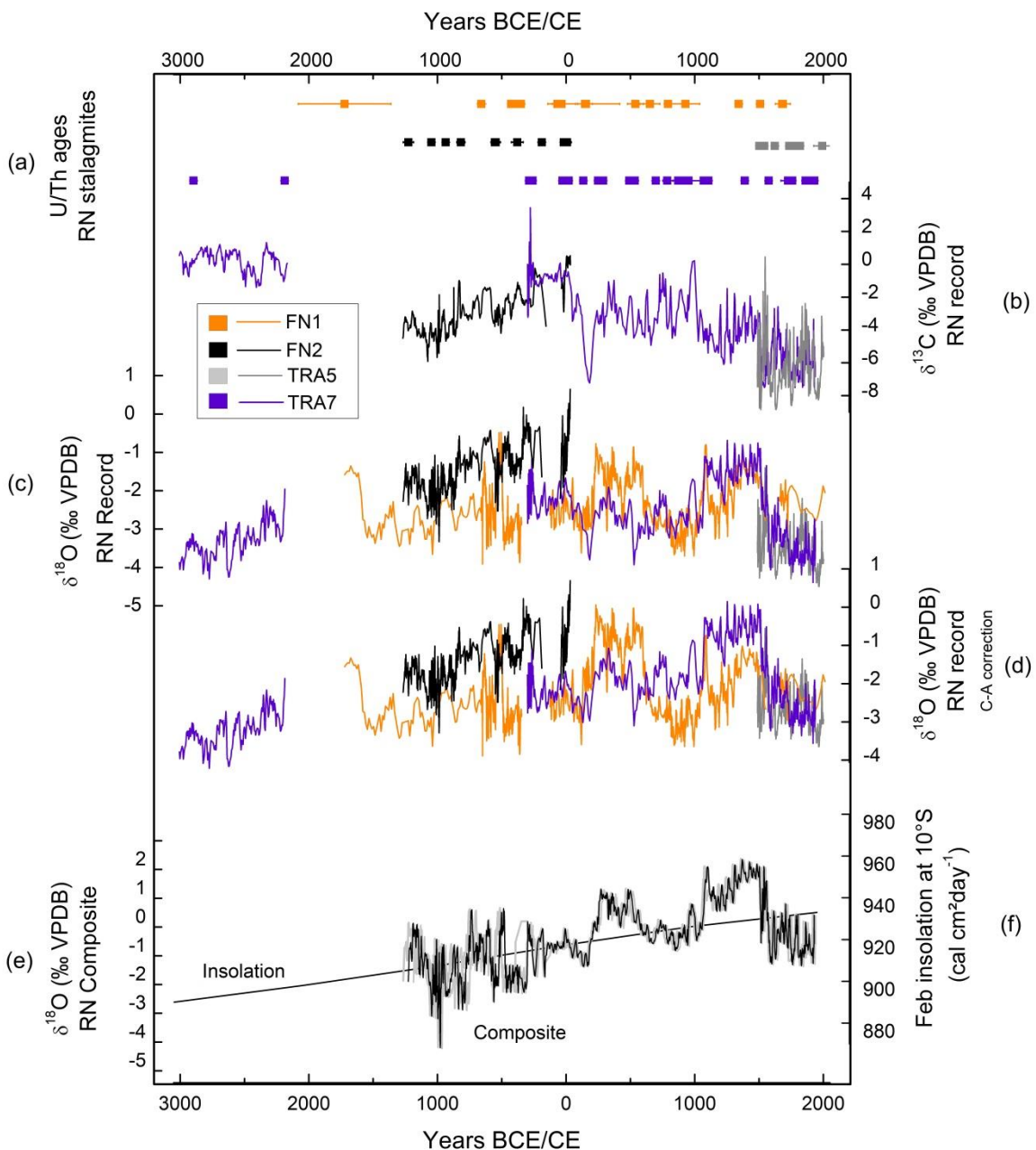
11
 12 Table S4 – Speleothem intervals according to texture and mineral weight proportion (wt).
 13 Texture description: A - crystals with mosaic and columnar fabrics; B - interbedded needle-like
 14 crystals. *Obtained by Utida et al. (2020). C-A: calcite-aragonite correction

Speleothem Mineralogy							
Sample	Interval (mm)	Age (yr BCE/CE)	Texture	Aragonite (wt %)	Calcite (wt %)	$\delta^{18}\text{O}$ mean (‰ VPDB)	
						before C-A correction	after C-A correction
TRA5	30-54	1745 to 1855 CE	A	0.0	100.0	-3.50	-2.65
	54-87	1640 to 1745 CE	A	0.0	100.0	-3.56	-2.71
	87-108	1565 to 1640 CE	A	0.0	100.0	-3.58	-2.73
	108-178	1490 to 1565 CE	A	0.0	100.0	-3.40	-2.55
TRA7*	0-173	130 BCE to 1940 CE	A	0.0	100.0	-2.80	-1.95
	173-215	290 to 130 BCE	B	99.0	1.0	-2.14	-2.13
	215-270	3000 to 290 BCE	B	87.1	12.9	-3.12	-3.01
FN1*	0-27	1170 to 1790 CE	B	85.2	14.9	-2.14	-2.01
	27-83	610 to 1170 CE	B	90.6	9.4	-2.87	-2.78
	83-128	80 to 610 CE	A	0.0	100.0	-1.87	-1.03
	128-202	1730 BCE to 80 CE	B	94.5	5.5	-2.54	-2.49
FN2	6-31	660 to 189 BCE	B	94.7	5.3	-1.20	-1.15
	31-56	960 to 660 BCE	B	94.8	5.2	-1.56	-1.52
	56-63	1005 to 960 BCE	B	94.8	5.2	-2.03	-1.99
	63-95	1265 to 1005 BCE	B	93.4	6.6	-1.94	-1.88



16

17 Figure S3 – Age models of each stalagmite from Rio Grande do Norte. Age models were
 18 calculated using COPRA (Breitenbach et al., 2012) through a set of 2.000 Monte Carlo simulations.
 19 The COPRA age model was produced for each sample and covers the entire stalagmite. Squares
 20 and horizontal bars: age results with error bars. Red line: COPRA average age model. Grey line:
 21 age model errors considering 95% confidence interval.

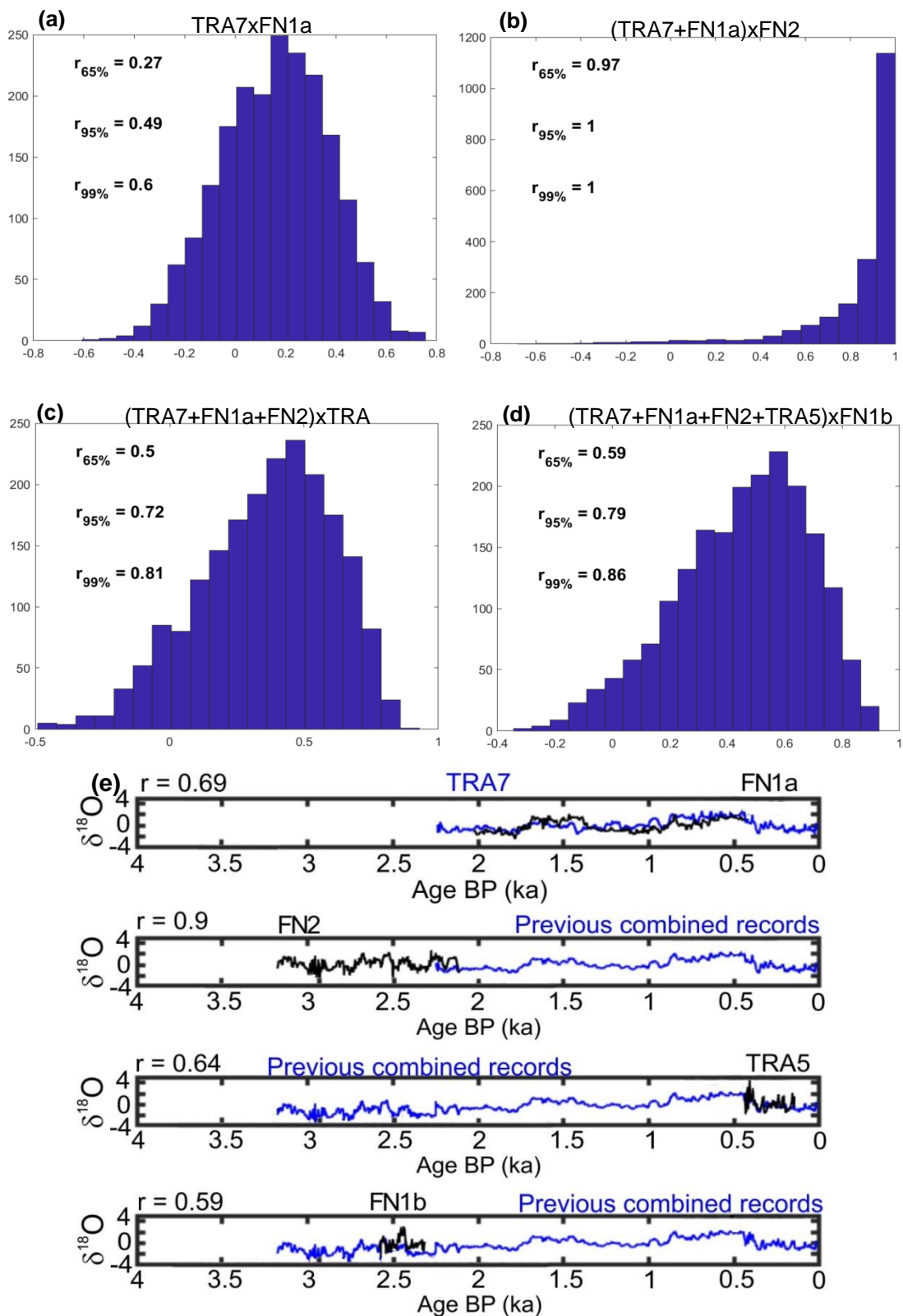


22

23

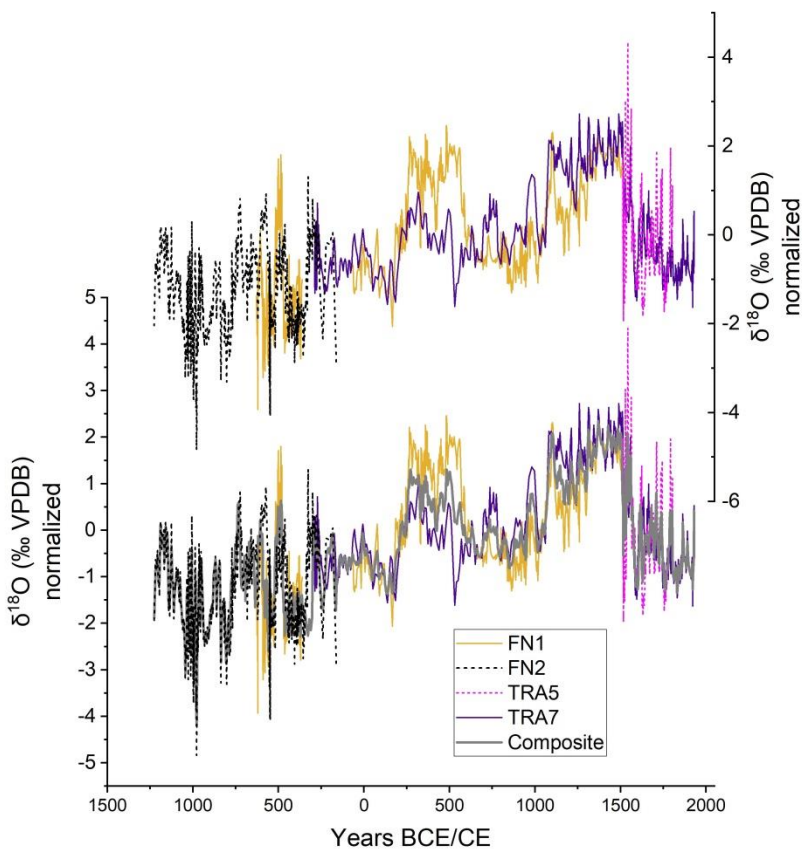
24 Figure S4 – Rio Grande do Norte stalagmite isotope record. (a) U/Th ages for RN
 25 stalagmites. (b) Raw data of $\delta^{13}\text{C}$. (c) Oxygen isotope results for RN record. (d) Oxygen isotope
 26 results corrected for calcite-aragonite fractionation ($\delta^{18}\text{O}_{\text{C-A}}$), according to weight proportion of
 27 mineralogical results. (e) $\delta^{18}\text{O}$ RN Composite constructed using stalagmite records from NEB
 28 (black line). Grey lines denote the age model confidence interval of 99%. (f) February insolation
 29 curve at 10°S (Berger and Loutre, 1991).

30



31

32 Figure S5 – Distribution of maximum correlation coefficients for 2000 pairs of AR1 time
 33 series with the same characteristics as the measured $\delta^{18}\text{O}$ stalagmite time series. a) distribution for
 34 TRA7 and FN1a; b) distribution for TRA7+FN1a and FN2; c) distribution for TRA7+FN1a+FN2 and
 35 TRA5; d) distribution for TRA7+FN1a+FN2+TRA5 and FN1b. e) Best time series results for the
 36 individual steps *iscam* performs for the composite time series construction. Highest correlation
 37 coefficient is indicated for each correlation step. All established time series are significant at the
 38 95% confidence limit.



39

40 Figure S6 – Oxygen isotopes plotted according to age model results calculated by ISCAM
 41 for RN record and RN Composite. The normalization of data is made by ISCAM (Fohlmeister,
 42 2012).

43

44 References

- 45 Berger, A., Loutre, M.F.: Insolation values for the climate of the last 10 million of years. Quat. Sci.
 46 Rev., 10, 297e317, [https://doi.org/10.1016/0277-3791\(91\)90033-Q](https://doi.org/10.1016/0277-3791(91)90033-Q), 1991.
- 47 Breitenbach. S.F.M., Rehfeld. K., Goswami. B., Baldini. J.U.L., Ridley. H. E., Kennett. D. J., Prufer.
 48 K.M., Aquino. V.V., Asmerom. Y., Polyak. V.J., Cheng. H., Kurths. J., Marwan. N.:
 49 COnstructing Proxy Records from Age models (COPRA), Clim. Past, 8, 1765–1779,
 50 <https://doi.org/10.5194/cp-8-1765-2012>, 2012.
- 51 Cheng, H., Edwards, R.L., Shen, C-C., Polyak, V.J., Asmerom, Y., Woodhead, J., Hellstrom, J.,
 52 Wang, Y., Kong, X., Spötl, C., Wang, X., Alexander Jr. E.C.: Improvements in ²³⁰Th dating,
 53 ²³⁰Th and ²³⁴U half-life values and U-Th isotopic measurements by multi-collector inductively
 54 coupled plasma mass spectrometry, Earth Planet. Sci. Lett., 371-372, 82-91,
 55 <https://doi.org/10.1016/j.epsl.2013.04.006>, 2013.
- 56 Cruz. F.W., Vuille. M., Burns. S.J., Wang. X., Cheng. H., Werner. M., Edwards. R.L., Karman. I.,
 57 Auler. A.S., Nguyen. H.: Orbitally driven east-west antiphasing of South American
 58 precipitation, Nat. Geosci., 2, 210-214, <https://doi.org/10.1038/ngeo444>, 2009.

- 59 Fohlmeister, J.: A statistical approach to construct composite climate records of dated archives,
60 Quat. Geochronol., 14, 48-56, <https://doi.org/10.1016/j.quageo.2012.06.007>, 2012.
- 61 Jaffey, A.H., Flynn, K.F., Glendenin, L.E., Bentley, W.C., Essling, A.M.: Precision measurement of
62 half-lives and specific activities of ^{235}U and ^{238}U , Physical Rev. C, 4, 1889-1906,
63 <https://doi.org/10.1103/PhysRevC.4.1889>, 1971.
- 64 Utida, G., Cruz, F.W., Santos, R.V., Sawakuchi, A.O., Wang, H., Pessenda, L.C.R., Novello, V.F.,
65 Vuille, M., Strauss, A.M., Borella, A.C., Stríkis, N.M., Guedes, C.C.F., De Andrade, F.D.,
66 Zhang, H., Cheng, H., Edwards, R.L.: Climate changes in Northeastern Brazil from deglacial to
67 Meghalayan periods and related environmental impacts, Quat. Sci. Rev., 250, 106655,
68 <https://doi.org/10.1016/j.quascirev.2020.106655>, 2020.
- 69 Zhang, H., Cai, Y., Tan, L., Qin, S., An, Z.: Stable isotope composition alteration produced by the
70 aragonite-to-calcite transformation in speleothems and implications for paleoclimate
71 reconstructions, Sediment. Geol., 309, 1-14, <https://doi.org/10.1016/j.sedgeo.2014.05.007>,
72 2014.